IEEE Access
Multidisciplinary | Rapid Review | Open Access Journal

Received 25 September 2022, accepted 18 October 2022, date of publication 25 October 2022, date of current version 4 November 2022.

Digital Object Identifier 10.1109/ACCESS.2022.3216775

RESEARCH ARTICLE

An Optimal Balanced Energy Harvesting Algorithm for Maximizing Two-Way Relaying D2D Communication Data Rate

MAHMOUD M. SALIM[1], HUSSEIN A. ELSAYED[2], (Member, IEEE), MOHAMED ABD ELAZIZ[3,4,5], MOSTAFA M. FOUDA[6], (Senior Member, IEEE), AND MOHAMED S. ABDALZAHER[7], (Senior Member, IEEE)

[1]Department of Electronics and Electrical Communications Engineering, October 6 University (O6U), Giza 12585, Egypt
[2]Department of Electronics and Electrical Communications Engineering, Ain Shams University (ASU), Cairo 11566, Egypt
[3]Department of Mathematics, Faculty of Science, Zagazig University, Zagazig 44519, Egypt
[4]Faculty of Computer Science and Engineering, Galala University, Suez 435611, Egypt
[5]Department of Electrical and Computer Engineering, Lebanese American University, Byblos 13-5053, Lebanon
[6]Department of Electrical and Computer Engineering, College of Science and Engineering, Idaho State University, Pocatello, ID 83209, USA
[7]Seismology Department, National Research Institute of Astronomy and Geophysics, Cairo 11421, Egypt

Corresponding author: Mahmoud M. Salim (m.salim.eng@o6u.edu.eg)

ABSTRACT Combining energy harvesting (EH) and device-to-device (D2D) communication underlaying 5G cellular networks is a very promising direction to improve both energy and spectral efficiencies. Unlike conventional relay-aided D2D communication that assumes one-way relaying (OWR) protocols, this paper proposes a two-way relaying (TWR) model. It aims to maximize the TWR D2D link rate that shares the uplink (UL) resources of the conventional cellular user (CU) considering the quality of service (QoS) constraints of all users. Besides, the relays are considered to harvest renewable energy (RE) from the ambient environment by relying on an attached solar panel. Also, they can harvest radio frequency (RF) energy from the received signal based on the power splitting (PS) EH protocol. Assuming that the UL resource allocation (RA) is already performed, the paper's objective is to jointly optimize the transmission power of all users in addition to the PS factor of relays based on the well-known meta-heuristic algorithm particle swarm optimization (PSO). Also, the best relay is selected by relying on the delimited area (DA) mechanism and the balanced residual energy (BRE) leading to TWR D2D link rate maximization and better energy efficiency (EE). The performance of the proposed algorithm is investigated through the results as well as comparing its performance to two of the most recent relay-aided D2D algorithms.

INDEX TERMS Device-to-device, two-way relaying, energy harvesting, power splitting, particle swarm optimization, power allocation, decode-and-forward, relay selection.

I. INTRODUCTION AND RELATED WORK

Device-to-device (D2D) communication is one of the most essential technologies in the 5G networks [1], [2]. It allows two nearby devices to directly communicate without the intervention from the base-station (BS) [3]. This direct communication underlaying conventional cellular network not only improves the network spectral efficiency (SE) but also its energy efficiency (EE) [4], [5], [6]. Since the resource sharing between the D2D and cellular links (CLs) imposes a serious mutual interference on both links, efficient resource and power allocation (PA) paradigms should be considered [7], [8].

Internet of things (IoT) has emerged with ubiquitous sensing and computing capabilities to interconnect thousands of physical devices to the Internet [9]. To facilitate our daily life, it comes with various applications such as vehicle-to-vehicle (V2V) communications, quality control, smart homes, and logistics and supply chain optimization [10], [11]. In this regard, machine learning and declustering can play a significant role [12], [13], [14], [15], [16], [17], [18], [19]. These applications coincides with new technologies such as

The associate editor coordinating the review of this manuscript and approving it for publication was Jie Tang.

machine learning, intelligent reconfigurable surface (IRS) and unmanned aerial vehicle (UAV) [20]. These technologies require high degree of image denoising for better service quality. Since the IoT terminals grow rapidly, IoT networks experience spectrum sharing shortages and EE limitations with unreliable quality of service (QoS) [21], [22], [23], [24], [25], [26], [27], [28], [29]. To cope with these problems, D2D communication appears as a key enabler technology to facilely realize the IoT application needs in terms of SE and EE [30], [31], [32].

To facilitate the collaboration among D2D users as well as utilize the cellular spectrum efficiently, the cooperative communications (CC) concept was presented [33], [34]. In the CC, two D2D terminals can share their data in a relay-aided manner through several intermediate cooperative relays [35], [36], [37], [38]. The majority of the literature focused on one-way relaying (OWR) D2D communication, where four phases are required to exchange messages between the two terminals. For instance, the authors in [39] proposed an OWR energy-efficient resource allocation (RA) scheme with optimal relay selection (RS) to improve the EE of the D2D communication, while the integration between OWR D2D communication and Non-orthogonal multiple access (NOMA) with optimal PA strategy to maximize the ergodic sum-rate was presented in [40]. However, the two-way relaying (TWR) approach needs only two phases which achieves higher throughput as well as lower power consumption [41], [42]. The authors in [43] investigated spectrum and energy efficiencies assumed amplify-and-forward (AF) TWR D2D communications underlaying cellular networks aimed at maximizing the D2D communication EE through optimal PA strategy. In [44], the SE of a decode-and-forward (DF) TWR D2D communication relying on the massive multiple-input multiple-output (MIMO) technology was proposed to improve the system SE. In [45], a new resource allocation scheme for D2D communication overlaying a cellular network was proposed. The scheme allowed the two terminals to perform D2D communication bidirectionally as well as assist the two-way communication between the BS and the cellular user (CU). An analytical approach to evaluate the TWR D2D communication performance with and without network coding was presented in [46] aimed to enhance the system throughput and end-to-end packet loss probability (E2EPLP).

Obviously, the participating relays not only do not get any individual benefit from participating in the relay-aided D2D link but also consume their own energy [47], [48]. Therefore, the energy harvesting (EH) concept can play an important role to compensate for this energy shortage and motivate the relays to participate [49], [50]. The relays can harvest energy either from renewable energy (RE) sources (e.g., solar) or from radio frequency (RF) signals [51], [52], [53]. The RF EH is performed based on the simultaneous wireless information and power transfer (SWIPT) technology that uses either time splitting (TS) or power splitting (PS) protocol [54], [55]. An EH relay-aided D2D communication that shares the DL resources of the conventional CUs considering the system QoS requirements was proposed in [49]. The authors presented a low complexity algorithm that can solve the problems of optimal RA, PS factor, and RS. In [56], a TWR D2D communication model underlaying cellular networks was proposed. The model assumed that the cooperative relays use the AF relaying protocol and can harvest the RF energy based on the TS protocol, where data transmission was performed in three time slots. The authors in [57] investigated a collaborative relay-aided D2D transmission paradigm with an EH feature for the relays. A rate-energy (R-E) region was also introduced to formulate a data rate maximization problem of the D2D pair, where the results showed that the data rate of the D2D pair was significantly improved. The RS in EH multihop D2D networks with an eavesdropper was investigated in [58] aimed at improving the secure connectivity performance of the relay. To achieve this, a source-to-destination secrecy connectivity probability (SCP) was derived showing a higher SCP of the proposed scheme than the direct transmission algorithms and conventional RS schemes in the simulation results.

A. MOTIVATION AND CONTRIBUTIONS

To the best of our knowledge, most of the previous works paid attention to a single TWR D2D communication issue such as EH considerations, PA, and RS. For example, the authors in [59] investigated the PA of a TWR AF-based D2D communication to maximize the D2D link rate without considering the RS and EH. Also, an optimal RS method was proposed in [60] ignoring PA and EH in their proposal. Accordingly, we have been motivated to present a TWR D2D communication model that shares the uplink (UL) spectrum of the conventional CUs considering a number of hybrid RF/RE-based EH relays (EHRs). The relays are assumed to harvest RF energy from the received signal based on the PS EH protocol. Also, they can harvest RE from the ambient environment relying on an attached solar panel. Since the EH capability can compensate for the relays' energy consumption, the relays are encouraged to cooperate and participate in the TWR D2D communication link. This comes with optimal PA, RS, and the amount of EH by the EHRs. It is worth noting that the RF harvested energy might not be enough for performing the D2D communication transmission. However, together with the RF energy, the RE can support the relay for further transmission.

This paper aims at maximizing the TWR D2D link rate while maintaining the required data rate of the CU assuming the RF/RE EH capabilities at the relays. Accordingly, a maximization problem is formulated as a mixed-integer nonlinear programming (MINLP) problem based on the assumption that the UL resources are already allocated by the BS. We aim to jointly optimize the transmission power of all users, the PS factor of relays, and the best relay to maximize the TWR D2D link rate. Therefore, a joint optimization algorithm called the joint PA and RS with EH (JPARS-EH) algorithm is proposed. The JPARS-EH algorithm optimally performs PA and PS factor optimization based on the well-known metaheuristic algorithm particle swarm optimization (PSO) as

well as optimal RS. To achieve balanced energy consumption, only relays that lie inside the delimited area (DA) and their residual energy above the average among the candidates can be nominated for selection namely the balanced residual energy (BRE). Besides, the proposed algorithm considers the power, QoS, and EH constraints.

Furthermore, the behavior of the JPARS-EH algorithm is investigated with respect to various parameters through the results. In addition, it is compared to the RPRS-EH algorithm presented in [49] and UL-*max* proposed in [61]. In contrast to the RPRS-EH and UL-*max* algorithms, the proposed algorithm utilizes the TWR transmission, which gives an advantage in terms of rate maximization. It is worth mentioning that the OWR model requires four phases for performing data transmission, while the TWR model needs only two phases. The proposed algorithm agrees with the UL-*max* that the delimited area (DA) mechanism for RS is used to limit the number of candidate relays. However, the UL-*max* is still an OWR model which cannot outperform our TWR model. Also, the UL-*max* algorithm aims at maximizing the D2D link rate ignoring the EE with no EH capabilities. Besides, the JPARS-EH utilizes the BRE that considers the relays' residual energy for RS together with the DA mechanism. This leads to TWR D2D link rate maximization and better EE.

For the RPRS-EH algorithm, it is an OWR algorithm that targets the relay-aided D2D link rate maximization by providing optimal RA, PA, and RS strategies as well as EE enhancement. This comes with assuming the RF/RE EH capability for the engaged relays. It is worth noting that the EH capability of OWR models provided by the RPRS-EH protocol cannot compete with that of the TWR model which is presented by our proposed model. Moreover, the BRE mechanism proposed in the RS strategy of the JPARS-EH algorithm gives more advantages in terms of fair energy distribution. The results show that the data rate and EE, in terms of harvested power, of our TWR proposal outperform the corresponding ones of the RPRS-EH algorithm.

In a nutshell, the main contributions of our work are summarized as the following:

- Assuming that the UL resources have been already allocated by the BS, a TWR D2D link rate MINLP maximization problem is formulated. This problem represents optimal PA, PS factor, and RS for the TWR D2D links underlaying conventional CUs. This comes with guaranteeing the maximum power limit of the sub-channels as well as the QoS and EH constraints.
- To solve this nonconvex problem, the JPARS-EH algorithm is proposed divided into two main sub-algorithms, namely, EHPA and BRMRS. Aiming at maximizing the TWR D2D link rate, the EHPA performs optimal PA relying on the PSO algorithm, while the BRMRS selects the best relay based on the DA mechanism besides the BRE concept. The BRE concept considers relays for selection whose residual energy is above the average among the candidates thus achieving balanced energy consumption.
- In the simulation results, the significance of the JPARS-EH algorithm is investigated showing a high degree of consistency concerning different parameters. Besides, the proposed algorithm outperforms both the two state-of-art OWR algorithms, namely, RPRS-EH and UL-*max*, in terms of D2D link rate. Also, the proposed algorithm gives better EE results in terms of harvested power when compared to the RPRS-EH scheme. Last but not least, the proposed algorithm with the BRMRS strategy shows better residual energy for candidate relays.

B. PAPER ORGANIZATION

The rest of this paper is organized as follows. In Section II, the system model is presented. Section III provides a brief explanation about the PSO algorithm, while the proposed algorithm JPARS-EH is discussed in Section IV. In Section V, the performance of the proposed algorithm is evaluated and compared to two of the most recent relay-aided algorithms. Finally, the conclusions of this paper are shown in Section VI.

II. SYSTEM MODEL

A cooperative UL resource sharing wireless network is considered in a single micro-cell, where a BS is geometrically located at the cell center. We consider two terminals, denoted by S_1 and S_2, that aim to exchange the information between each other through the assist of multiple EHRs. These EHRs are randomly located within the two terminals' communication range and each relay is denoted by R_l, $l \in \{1, 2, \ldots, L\}$. In addition, it is assumed that each EHR is a half-duplex and self-powered relay with TWR capability.

A number of cellular and D2D links are assumed, which are denoted by $\mathbf{K} = \{1, 2, \ldots, K\}$ and $\mathbf{M} = \{1, 2, \ldots, M\}$, respectively. The communication channels among the links are independent and identically distributed (i.i.d.) Rayleigh channels considering the perfect channel state information (CSI) availability. Due to the communication channels' rapid change, the imperfect CSI is more realistic for defining them. In order to deal with the time variance and frequency selectivity of wireless channels and to minimize the channel estimate error, a channel estimation technique is required [62]. In fact, the resulting channel attenuation from the imperfect CSI lowers the system data rate and, as a result, lowers the system EE [63]. To solve this issue, unique resources and PA algorithms are required. To avoid deviating from the primary goal of our paper, we make the assumption that the perfect CSI will postpone the effects of the imperfect CSI for future work, similar to many earlier publications [49], [64].

Without loss of generality, the subscripts c and b denote the CU and BS, respectively, while the subscripts s_1 and s_2 denote the first and second terminal, respectively. Also, the EHR l is denoted by r_l. For example, $h_{s_1 r_l}$ and $d_{s_1 r_l}$ are used to define the channel attenuation coefficient and distance between the terminal S_1 and the relay R_l. Thus the channel gain between them is:

$$\alpha_{s_1 r_l} = \frac{|h_{s_1 r_l}|^2}{d^v_{s_1 r_l}}, \tag{1}$$

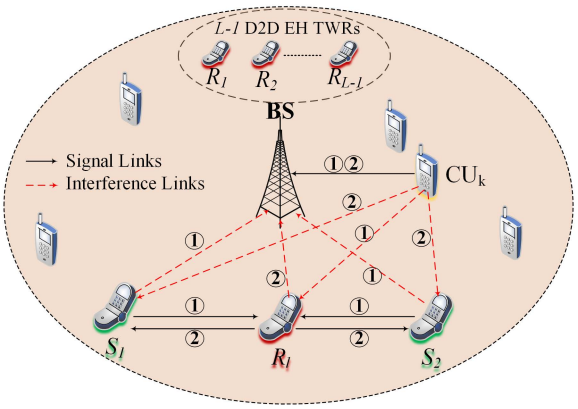

FIGURE 1. System model of the TWR D2D communication underlaying conventional UL cellular network.

where ν represents the path loss exponent. In addition, σ^2 is used to denote the noise power.

Assuming a TWR communication system, the data transmission time is performed in W time slots. Each time slot w of duration T_c consists of two sub-slots (i.e., δ_1 and δ_2), where the sub-slot duration is $\frac{T_c}{2}$. During δ_1, which is known as the multiple access phase (MAP), the CU transmits its message to the BS, while S_1 and S_2 transmit their messages to the TWR relay R_l. During δ_2, which is called the broadcast phase (BP), the CU again sends its data to the BS, while R_l broadcasts the signal back to the terminals S_1 and S_2 using the DF strategy [65].

It is worth noting that the relay R_l is equipped with two energy harvesters. One of them is an RF energy harvester that is capable of harvesting energy from received power. However, the other harvester can harvest the RE energy from the ambient environment. In addition, the proposed model assumes that the TWR links share the same UL spectrum of the CLs considering a set of N sub-channels that is denoted as $\mathbf{N} = \{1, 2, ..., N\}$. In this paper, it is assumed that the UL resources are already allocated to the CUs and utilized by the TWR links in an underlay mode. Thus, the D2D users can simultaneously use the resources of the CUs feasibly. A scenario of selecting a TWR link $m \in \mathbf{M}$ that contains relay l underlying a CL $k \in \mathbf{K}$, where both of them share the same sub-channel $n \in \mathbf{N}$ is depicted in Figure 1. Besides, all the considered notations in this paper are illustrated in Table 1.

A. TRANSMISSION MODEL

The proposed model assumes one TWR link m among the available M links considering the PS protocol for the relays' RF EH. In the PS protocol, the relay uses a fraction of the received signal for EH. However, the remaining part is used for information decoding. It is worth noting that the RF energy only assists for the relay node's (RN) transmission, while the relay mainly depends on the RE due to its large value when compared to the RF energy. The importance of the RE for supporting the relay's transmission is illustrated in Section IV-A.

As aforementioned, the data transmission of each time slot w is performed in two phases, which are the MAP and BP.

TABLE 1. List of notations.

Symbol	Description
$\mathbf{K}$	Set of cellular links
$\mathbf{M}$	Set of TWR D2D links
$\mathbf{N}$	Set of sub-channels
P_c	Transmit power of cellular user k
P_{s_1}	Transmit power of terminal S_1
P_{s_2}	Transmit power of terminal S_2
P_{r_l}	Transmit power of relay l
$E^{RE}_{r_l}$	Instantaneous RE amount at relay l
$E^{RF}_{r_l}$	Instantaneous RF energy amount at relay l
$E^{h}_{r_l}$	Total energy harvested by relay l
$E^{Res}_{r_l}$	Residual energy of relay l
$E^{C}_{r_l}$	Energy consumption of relay l
T_c	Time slot duration
h_{ab}	Channel attenuation coefficient between node a and b
d_{ab}	Distance between node a and b
α_{ab}	Channel gain between node a and b
$\boldsymbol{G}$	Channel gain matrix
x_{ab}	Transmitted message between node a and b
Y_{ab}	Received message between node a and b
ν	Path loss exponent
R_l	Two-way EH relay l (EHR)
$\mathcal{R}_\psi$	Selected EH relay ($l = \psi$)
β_{mr_l}	Relay selection binary variable
ρ_{r_l}	PS ratio of R_l (if R_l is selected, $l = \mathcal{S}$)
η^{RF}	RF conversion efficiency coefficient
$\mathcal{N}$	Number of PSO solutions
c_1 and c_2	PSO acceleration coefficients
Dim	Number of dimensions for each PSO solution
T_{max}	PSO maximum number of iterations

During the MAP (i.e., δ_1), the received signal and the signal-to-interference-noise ratio (SINR) at the BS are respectively given by:

$$Y^{(\delta_1)}_{b,w} = \sqrt{P_{c,w}}\frac{h_{cb,w}}{\sqrt{d^{\nu}_{cb,w}}}x_{cb,w} + \sqrt{P_{s_1,w}}\frac{h_{s_1b,w}}{\sqrt{d^{\nu}_{s_1b,w}}}x_{s_1r_l,w} + \sqrt{P_{s_2,w}}\frac{h_{s_2b,w}}{\sqrt{d^{\nu}_{s_2b,w}}}x_{s_2r_l,w} + n_{b,w}, \tag{2}$$

$$\gamma^{(\delta_1)}_{b,w} = \frac{P_{c,w}\alpha_{cb,w}}{P_{s_1,w}\alpha_{s_1b,w} + P_{s_2,w}\alpha_{s_2b,w} + \sigma^2}, \tag{3}$$

where $P_{c,w}$ is the CU transmission power, while $n_{b,w}$ is the AWGN and conversion combined noise at the BS. The $P_{s_1,w}$ and $P_{s_2,w}$ are the transmission power of terminal S_1 and S_2, respectively.

The received signal at the relay R_l can be expressed as follows:

$$Y^{(\delta_1)}_{r_l,w} = \sqrt{(1-\rho_{r_l,w})P_{s_1,w}}\frac{h_{s_1r_l,w}}{\sqrt{d^{\nu}_{s_1r_l,w}}}x_{s_1r_l,w} + \sqrt{(1-\rho_{r_l,w})P_{s_2,w}}\frac{h_{s_2r_l,w}}{\sqrt{d^{\nu}_{s_2r_l,w}}}x_{s_2r_l,w} + \sqrt{P_{c,w}}\frac{h_{cr_l,w}}{\sqrt{d^{\nu}_{cr_l,w}}}x_{cb,w} + n_{r_l,w}, \tag{4}$$

where $\rho_{r_l,w}$ is the PS factor of R_l to be optimized during time slot w. The part of the received signal that is used for information decoding is denoted by $(1-\rho_{r_l,w})\left(P_{s_1,w}\alpha_{s_1r_l,w}+P_{s_2,w}\alpha_{s_2r_l,w}\right)$. However, the remaining part that is used for relay $l's$ EH is $\rho_{r_l,w}\left(P_{s_1,w}\alpha_{s_1r_l,w}+P_{s_2,w}\alpha_{s_2r_l,w}\right)$. This energy amount is stored in the relay's battery to be used during δ_2 transmission. It is worth noting that the RF harvested energy might not be enough for performing the BP transmission. However, together with the RF energy, the RE can support the relay transmission during the second phase. We assume that the noise power is not considered for harvesting due to its tiny value [49] in addition to the CU interference due to its far position. The SINR of the S_1-R_l and S_2-R_l links are given respectively as:

$$\gamma^{(\delta_1)}_{s_1r_l,w}=\frac{(1-\rho_{r_l,w})P_{s_1,w}\alpha_{s_1r_l,w}}{P_{c,w}\alpha_{cr_l,w}+\sigma^2}, \tag{5}$$

$$\gamma^{(\delta_1)}_{s_2r_l,w}=\frac{(1-\rho_{r_l,w})P_{s_2,w}\alpha_{s_2r_l,w}}{P_{c,w}\alpha_{cr_l,w}+\sigma^2}. \tag{6}$$

During the BC phase (i.e., δ_2), the received signal and SINR at the BS are respectively given as the following:

$$Y^{(\delta_2)}_{b,w}=\sqrt{P_{c,w}}\frac{h_{cb,w}}{\sqrt{d^v_{cb,w}}}x_{cb,w}+\sqrt{P_{r_l,w}}\frac{h_{r_lb,w}}{\sqrt{d^v_{r_lb,w}}}Y^{(\delta_1)}_{r_l,w}+n_{b,w}, \tag{7}$$

$$\gamma^{(\delta_2)}_{b,w}=\frac{P_{c,w}\alpha_{cb,w}}{P_{r_l,w}\alpha_{r_lb,w}+\sigma^2}. \tag{8}$$

The received signal at terminal S_1 and terminal S_2 are respectively given as:

$$Y^{(\delta_2)}_{r_ls_1,w}=\sqrt{P_{r_l,w}}\frac{h_{r_ls_1,w}}{\sqrt{d^v_{r_ls_1,w}}}x_{r_ls_1,w}+\sqrt{P_{c,w}}\frac{h_{cs_1,w}}{\sqrt{d^v_{cs_1,w}}}x_{cb,w}+n_{s_1,w}, \tag{9}$$

$$Y^{(\delta_2)}_{r_ls_2,w}=\sqrt{P_{r_l,w}}\frac{h_{r_ls_2,w}}{\sqrt{d^v_{r_ls_2,w}}}x_{r_ls_2,w}+\sqrt{P_{c,w}}\frac{h_{cs_2,w}}{\sqrt{d^v_{cs_2,w}}}x_{cb,w}+n_{s_2,w}. \tag{10}$$

Furthermore, the SINR at terminal S_1 and terminal S_2 are respectively given as follows:

$$\gamma^{(\delta_2)}_{r_ls_1,w}=\frac{P_{r_l,w}\alpha_{r_ls_1,w}}{P_{c,w}\alpha_{cs_1,w}+\sigma^2}, \tag{11}$$

$$\gamma^{(\delta_2)}_{r_ls_2,w}=\frac{P_{r_l,w}\alpha_{r_ls_2,w}}{P_{c,w}\alpha_{cs_2,w}+\sigma^2}. \tag{12}$$

B. RELAY ENERGY HARVESTING MODEL

Each relay R_l is assumed to be equipped with two energy harvesters. One of them is an RF energy harvester that is capable of harvesting energy from the received power based on the PS protocol. However, the other harvester can harvest the RE from the ambient environment. Figure 2 shows the two energy sources that play an important role for charging the relay's battery, where R_l is denoted R_S when selected. Since each selected relay R_l (i.e., $l=\psi$) is considered as a TWR EHR, its transmission power P_{r_l} mainly depends on the RF and RE harvested from the ambient environment. Thus, we can define the amount of the EH by R_l at the beginning of each time slot w as follows:

$$\begin{aligned}E^h_{r_l,w}&=E^{RF}_{r_l,w}+E^{RE}_{r_l,w}\\&=\beta^{(n)}_{mr_l,w}\left[\frac{T_c}{2}\eta^{RF}\rho_{r_l,w}\left(P_{s_1,w}\alpha_{s_1r_l,w}+P_{s_2,w}\alpha_{s_2r_l,w}\right)\right]\\&\quad+E^{RE}_{r_l,w},\end{aligned} \tag{13}$$

where η^{RF} is the conversion efficiency coefficient of the RF source, $\rho_{r_l,w}$ is the PS EH factor, and $E^{RE}_{r_l,w}$ refers to the amount of RE EH by relay l. The binary variable $\beta^{(n)}_{mr_l,w}$ refers to the l^{th} relay condition to be selected or non-selected to participate in the TWR D2D link m transmission during time slot w using sub-channel n. If R_l is selected, $\beta^{(n)}_{mr_l,w}=1$; otherwise, $\beta^{(n)}_{mr_l,w}=0$. It is clear from (13) that each relay performs RE harvesting if it is selected or not. This energy amount supports the relay's future transmission and motivates it for participation. Following the real-life data set of the National Renewable Energy Laboratory (NREL), the day time mean and variance solar EH are $0.024W=m^2$ and $4.3W=m^2$, respectively. These values are the considered values of our model [49], [66]. Besides, this paper takes into consideration the harvest-store-use transmission management paradigm with negligible energy storage and retrieval from the battery [41]. Furthermore, the EH overflow and causality constraints are considered [49].

At the end of each time slot w, the relay R_l can determine its residual energy which is obtained from the EH during the current time slot w in addition to the residual energy of $w-1$ as follows:

$$\begin{aligned}E^{Res}_{r_l,w}=\min\Big\{E_{max},\Big(&\beta^{(n)}_{mr_l,w}[E^{Res}_{r_l,w-1}+E^h_{r_l,w}-E^C_{r_l,w}]\\&+(1-\beta^{(n)}_{mr_l,w})[E^{Res}_{r_l,w-1}+E^h_{r_l,w}]\Big)\Big\},\end{aligned} \tag{14}$$

where $E^C_{r_l,w}$ denotes the amount of energy that R_l consumes when selected during the current time slot w.

C. D2D RATE FORMULA

From equations (5), (6), (11), and (12), according to the DF protocol consideration, the following equations can be obtained [65]:

$$R_{s_1r_l}=\frac{1}{2}\log_2\left(1+\gamma^{(\delta_1)}_{s_1r_l,w}\right), \tag{15}$$

$$R_{s_2r_l}=\frac{1}{2}\log_2\left(1+\gamma^{(\delta_1)}_{s_2r_l,w}\right), \tag{16}$$

$$R_{r_ls_1}=\frac{1}{2}\log_2\left(1+\gamma^{(\delta_2)}_{r_ls_1,w}\right), \tag{17}$$

$$R_{r_ls_2}=\frac{1}{2}\log_2\left(1+\gamma^{(\delta_2)}_{r_ls_2,w}\right), \tag{18}$$

$$R_{MA}=\frac{1}{2}\left(1+\left[\gamma^{(\delta_1)}_{s_1r_l,w}+\gamma^{(\delta_1)}_{s_2r_l,w}\right]\right), \tag{19}$$

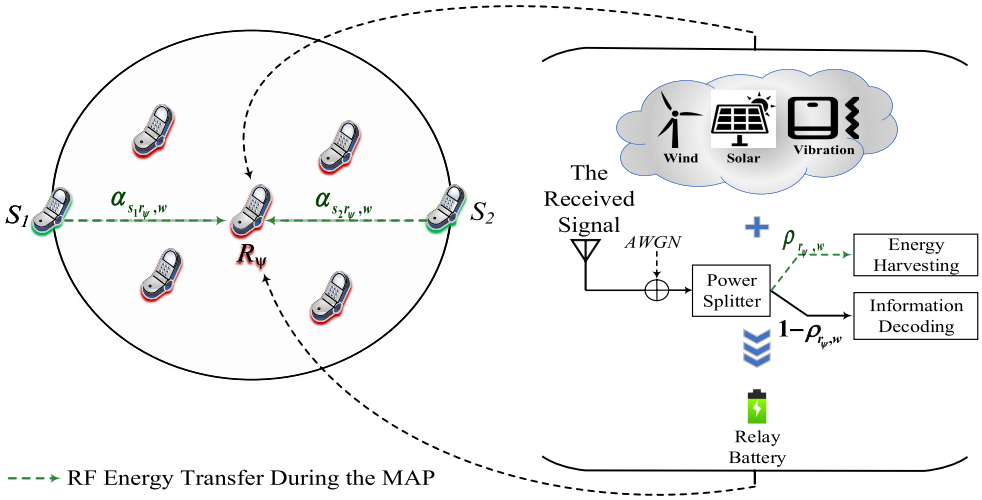

FIGURE 2. The EH model of an EHR when selected.

where R_{MA} denotes the multiple access information transfer rate as the achievable TWR D2D link rate is the smaller of the sum of the end-to-end rates and the MA rate. Therefore, the TWR D2D link rate can be expressed as follows:

$$\begin{aligned} R^D_{Sum} &= R_{s_1 s_2} + R_{s_2 s_1} \\ &= \min\left(R_o, R_1, R_2, R_3, R_4\right), \end{aligned} \tag{20}$$

where $R_o = R_{s_1 r_l} + R_{s_2 r_l}$, $R_1 = R_{s_1 r_l} + R_{r_l s_1}$, $R_2 = R_{r_l s_2} + R_{s_2 r_l}$, $R_3 = R_{r_l s_1} + R_{r_l s_2}$, and $R_4 = R_{MA}$.

D. PROBLEM FORMULATION

Here, we formulate the problem of TWR D2D communication links underlaying conventional CLs using the UL spectrum sharing with RE/RF EH capability for the participating relays.

We aim at maximizing the TWR D2D link rate with conserving the CL rate requirements. This can be achieved by optimally allocating the power for the two links such that the TWR D2D link rate is maximized taking into account the power constraints. Also, the optimal PS factor for the relay should be adaptively determined. In addition, the EHR that maximizes the TWR D2D link data rate is supposed to be selected based on the DA and BRE mechanisms. Moreover, the maximum practical transmission power of the sub-channels should be taken into account. Besides, the EH and the QoS constraints of both the cellular and TWR D2D links should be considered. Whereas, the assignment of only one sub-channel for each CL should be guaranteed. The optimization problem can be formulated as a constrained objective function as follows:

$$\max_{\rho_{r_l}, P_{s_1}, P_{s_2}, P_{r_l}, P_c, U^{(n)}_{mk}, \beta^{(n)}_{mr_l}} \sum_{m \in \mathbb{M}} R^D_{sum}, \tag{21a}$$

$$\text{subject to:} \sum_{m=1}^{M} \sum_{k=1}^{K} U^{(n)}_{mk,w} \leq 1 \quad \forall n, \tag{21b}$$

$$\text{where} \quad U^{(n)}_{mk,w} = \{0, 1\}, \quad \forall k, m, n,$$

$$0 \leq \rho_{r_l, w} \leq 1, \quad \forall l, \tag{21c}$$

$$\min \quad \{\gamma^{(\delta_1)}_{b,w}, \gamma^{(\delta_2)}_{b,w}, \gamma^{(\delta_1)}_{s_1 r_l, w}, \gamma^{(\delta_1)}_{s_2 r_l, w}, \gamma^{(\delta_2)}_{r_l s_1, w}, \gamma^{(\delta_2)}_{r_l s_2, w}\} \tag{21d}$$

$$\geq \gamma_{min}, 0 \leq P^{(n)}_{i,w} \leq P_{max},$$

$$\text{where} \quad i \in \{c, s_1, s_2, r_l\}, \quad \forall t, l, n, , \tag{21e}$$

$$\sum_{m=1}^{M} \sum_{l=1}^{L} \beta^{(n)}_{mr_l, w} \leq 1,$$

$$\text{where} \quad \beta^{(n)}_{mr_l, w} = \{0, 1\}, \quad \forall l, m, n,$$

$$P^{(n)}_{j,w} \frac{T_c}{2} \leq E^h_{j,w} + E^{Res}_{j,w-1} \tag{21f}$$

$$\text{where} \quad j \in \{s_1, s_2, r_l\}, \quad \forall l, n, \tag{21g}$$

$$E^{Res}_{j,w} \leq E_{max} \quad \forall l, \tag{21h}$$

where (21a) depicts the main OF that aims at maximizing the TWR D2D links data rate. Constraint (21b) guarantees that only one sub-channel n is shared between the TWR D2D and CLs. Whereas, constraint (21c) shows the interval in which the PS factor optimal value lies for the participating relay l. Moreover, constraint (21e) is added to ensure that all the links achieve a minimum required SINR value γ_{min}. In addition, it is depicted in constraint (21e) that the practical transmit powers of all links are always within the maximum power limit P_{max}. In constraint (21f), it is shown that each TWR D2D link includes only one relay R_l that shares a single sub-channel n. Constraints (21g) depicts the energy causality constraint, while constraint (21h) depicts the energy overflow constraint.

Since (21a) represents an MINLP problem that includes (21a) which is a non-convex OF, the problem is considered as an NP-hard problem that cannot be solved in a straightforward manner [49]. As aforementioned, the UL resources are assumed to be allocated to the CUs and utilized by the TWR links in an underlay mode, where a novel RA scheme can be presented in the future work. So, we decompose the main

problem into two sub-problems and present an efficient algorithm that is able to solve the two sub-problems separately.

III. PARTICLE SWARM OPTIMIZATION ALGORITHM

In this section, the basic concepts of the PSO are discussed [67]. Since the PSO efficiently contributed to solving many of the PA problems [35], [64], it is the key tool for jointly optimizing the users' transmission powers and the relays' PS factors. In general, the PSO is a swarm technique that simulates the social behavior of birds and how they communicate together. The PSO begins by determining the position and velocity of each of $\mathcal{N}$ particles/solutions (i.e., x_i and v_i). The next step is to check the quality of these solutions by computing the fitness value (F_b) and determining the best position for each particle $x_i^{p(t)}$ as well as the global best position $x_j^{g(t)}$. Then, the PSO updates the position of each particle using the following equations:

$$x_i^{(t+1)} = x_i^{(t)} + v_i^{(t+1)}, \tag{22}$$

$$v_i^{(t+1)} = wv_i^{(t)} + c_1 r_1 (x_i^{p(t)} - x_i^{(t)}) + c_2 r_2 (x_j^{g(t)} - x_i^{(t)}), \tag{23}$$

where t is the current iteration, w represents an inertia weight that is used to enhance the convergence speed. c_1 and c_2 are the acceleration coefficients, while r_1 and r_2 represent the random parameters $\in [0, 1]$.

The previous steps are repeated until meeting the terminal conditions (see Algorithm 1).

Algorithm 1 Particle Swarm Optimization Algorithm (PSO)

Input: $\mathcal{N}$ Number of solutions, lower and upper boundaries.

1: Initialize a set of positions and velocities.
2: **repeat**
3: **for** $i = 1 : \mathcal{N}$ **do**
4: Compute the fitness value for x_i.
5: Determine the best personal solution $x_i^{p(t)}$ and global best $x_j^{g(t)}$.
6: Update the velocity using Eq.(22).
7: Update the position Eq.(23).
8: Check the lower and upper boundaries.
9: **end for**
10: **until** stop conditions are met

Output: Return the best solution.

IV. JOINT POWER ALLOCATION AND RELAY SELECTION WITH ENERGY HARVESTING ALGORITHM (JPARS-EH)

In this section, our problem is divided into two main sub-problems. The first one is to optimally allocate the power for each link by determining the optimal PS factor value for the relays. The second sub-problem is to optimally select the best RN among the existing based on the DA and BRE mechanisms. It is worth noting that the two sub-problems share the same aim, which is maximizing the TWR D2D data rate. For solving these two sub-problems, the JPARS-EH algorithm that is divided into two main sub-algorithms is presented. Each sub-algorithm can solve one of the aforementioned sub-problems as follows.

A. ENERGY HARVESTING POWER ALLOCATION SUB-ALGORITHM (EHPA)

Here, the EHPA sub-algorithm is presented. It can optimally allocate the transmission powers for all transmitters including the cellular user (i.e.P_c) and D2D users (i.e.$P_{s_1}, P_{s_2}, P_{r_l}$). In addition, it determines the optimal value of the PS factor for each relay (i.e., ρ_{r_l}). These power and PS factor optimizations are performed based on the PSO algorithm which first determines the boundaries of its parameters $P_{s_1}, P_{s_2}, P_{r_l}$, and ρ_{r_l}. Then, the PSO selects the best values of these parameters that optimize the data rate. Furthermore, the EHPA sub-algorithm takes into account the QoS constraints represented by (21e) as well as the EH causality constraints of the relays as in (21g). Since the CU has the priority in such communication models, it is allocated the maximum power limit (i.e., $P_c = P_{max}$). This guarantees that the QoS requirements of the CU are not negatively affected.

Clearly, for fixed sub-channels, the EHPA sub-problem can be written as:

$$\max_{\rho_{r_l}, P_{s_1}, P_{s_2}, P_{r_l}} \sum_{m \in \mathbb{M}} R_{sum}^D, \tag{24a}$$

$$\text{subject to (21c), (21e), (21e), and (21g).} \tag{24b}$$

The solution of the EHPA sub-problem can be achieved relying on the PSO algorithm in two steps. First, the lower and upper boundaries of the optimization parameters are deduced followed by the optimization step as the follows:

1) BOUNDARIES DETERMINATION

The optimization parameters that need to be optimized are $\rho_{r_l}, P_{s_1}, P_{s_2}$, and P_{r_l}. The lower and upper boundaries of these parameters should be determined in order to search for an optimal solution. It is clear that (21c) represents the lower and upper boundaries of the PS factor. In order to guarantee the minimum SINR requirements of the $S_1 - R_l$ and $S_2 - R_l$ links, we substitute in (5) and (6) with γ_{min} so we can obtain the two power lower boundaries of S_1 and S_2 respectively as follows:

$$P_{s_1 Low} = \frac{\gamma_{min}(P_{c,w}\alpha_{cr_l,w} + \sigma^2)}{(1 - \rho_{r_l,w})\alpha_{s_1 r_l,w}}, \tag{25}$$

$$P_{s_2 Low} = \frac{\gamma_{min}(P_{c,w}\alpha_{cr_l,w} + \sigma^2)}{(1 - \rho_{r_l,w})\alpha_{s_2 r_l,w}}. \tag{26}$$

Similarly, by substituting in (3) with γ_{min}, we can get the upper power boundary of S_1 which is assumed to be equal to that of S_2 as follows:

$$P_{s_1 High} = P_{s_2 High} = \max \left\{ P_{max}, \left(\frac{1}{\alpha_{s_1 b,w} + \alpha_{s_2 b,w}} \right) \left(\frac{P_{c,w}\alpha_{cb,w}}{\gamma_{min}} - \sigma^2 \right) \right\}, \tag{27}$$

where P_{max} ensures the maximum practical power limit of S_1 and S_2. It is important to note that $P_{s_1 High}$ and $P_{s_2 High}$

maintain the minimum SINR requirements of the CU during δ_1.

In order to obtain the lower boundary of the relay power during δ_2, we take the maximum value of the two values that yield from the substitution of γ_{min} in (11) and (12). Hence, the lower boundary of P_{r_l} is given by:

$$P_{r_l Low} = \max\left\{\frac{\gamma_{min}[P_{c,w}\alpha_{cs_1,w} + \sigma^2]}{\alpha_{r_l s_1,w}}, \frac{\gamma_{min}[P_{c,w}\alpha_{cs_2,w} + \sigma^2]}{\alpha_{r_l s_2,w}}\right\}. \quad (28)$$

In the same way, we can obtain the upper boundary of the relay transmission power from (8) as follows:

$$P_{r_l High} = \max\left\{P_{max}, P^{Res}_{r_l,w}, \frac{P_{c,w}\alpha_{cb,w} - \gamma_{min}\sigma^2}{\gamma_{min}\alpha_{r_l b,w}}\right\}, \quad (29)$$

where P_{max} ensures the maximum practical power limit of the relay R_l at time slot w, while $P^{Res}_{r_l,w} = T_c E^{Res}_{r_l,w}$ ensures the causality constraint of the same relay at the same w. It can be observed that (28) guarantees the minimum SINR requirements of $R_l - S_t$ during δ_2, while (29) guarantees that of the CL during δ_2.

2) PSO Optimization

After the boundaries' determination, the PSO starts to receive the input values such as the number of solutions $\mathcal{N}$ in addition to the lower and the upper boundaries for each parameter. Since we have four parameters that should be optimized, the dimension field of each solution is set to four ($Dim = 4$). The first value of the solution represents ρ_{r_l}, while the second, third, and fourth value represents P_{s_1}, P_{s_2}, and P_{r_l}, respectively. After that, the PSO computes F_b for each solution using (24a) followed by the step of determining the best personal solution x^p and the global best solution x^g. Next, the current solutions are updated using (22) and (23). Then, the lower and upper boundaries of each solution are checked. Clearly, the previous steps are repeated until the stop conditions are met then the best solution which represents the values for the parameters ρ_{r_l}, P_{s_1}, P_{s_2}, and P_{r_l} is returned. The details of the EHPA strategy are illustrated in Sub-algorithm 2.

B. BALANCED RATE MAXIMIZATION RS SUB-ALGORITHM (BRMRS)

In this subsection, an RS sub-algorithm namely the BRMRS is presented. The BRMRS sub-algorithm is capable of selecting the optimal relay that maximizes the TWR D2D link rate. As explained in the EHPA sub-algorithm, the optimal powers are allocated for each TWR D2D link m so each link can decide which relay to be selected for its rate maximization. Obviously, the optimal relay should lie in the area that is located between S_1 and S_2. Thus, the BRMRS scheme performs the optimal RS relying on the DA mechanism [61]. To reduce the number of nominated relays, two circles with radius $d_{S_1S_2}$ are formed, which centers are S_1 and S_2. The intersection between the two circles is called the DA, which

Sub-Algorithm 2 Energy Harvesting Power Allocation Sub-Algorithm (EHPA)

Input: η^{RF}, P_{max}, γ_{min}, $\rho_{r_l,w} \in [0, 1]$, $\boldsymbol{G}$, T_{max}.
Output: $\rho^{opt}_{r_l,w}$, $P^{opt}_{s_1,w}$, $P^{opt}_{s_2,w}$, $P^{opt}_{r_l,w}$, $\forall l$.

1: **Initialize:** $P_{c,w} = P_{max}$, $t = 1$.
2: **Step 1:Boundaries Determination**
3: Determine the lower and upper boundaries of the parameters $P_{s_1,w}$, $P_{s_2,w}$, $P_{r_l,w}$ according to (25) to (29).
4: **Step 2: PSO Optimization**
5: Set the initial value for $\mathcal{N}$ solutions.
6: **while** $t \leq T_{max}$ **do**
7: Check the boundaries of each solution x_i using (25) to (29).
8: Compute the fitness value F_b as defined in (21a).
9: Determine the best personal solution x^p and the global solution x^g.
10: Update the solutions using (22) and (23).
11: $t = t + 1$.
12: **end while**
13: Return the optimal solution.

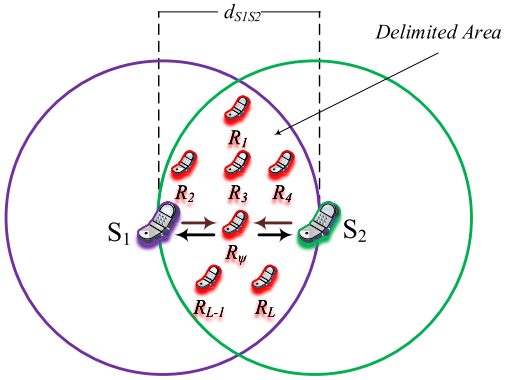

FIGURE 3. Optimal RS in the BRMRS sub-algorithm.

is the area used for RS (see Figure 3). Utilizing the DA mechanism limits the number of candidate relays for optimal relay selection, which reduces the algorithm complexity. The BRMRS not only considers the data rate maximization but also considers the energy consumption fairness among the candidate relays to achieve high EE. This can be achieved by selecting the best relay among the candidates lying inside the DA with residual energies above the average, obeying the BRE concept, thus achieving balanced energy consumption.

For fixed sub-channels and optimally allocated powers, the RS sub-problem can be written as:

$$\mathcal{R}_\psi = \max_{\beta_{mr_l,w}} \sum_{m\in\mathbb{M}} R^D_{sum}, \quad (30a)$$

$$\text{subject to (21f) and (21h)}, \quad (30b)$$

where $\mathcal{R}_\psi$ denotes the selected relay that achieves the maximum TWR D2D data rate among the others with residual energy above the average. After the RS process, the residual energy is calculated according to (14) considering the overflow constraint represented by (21h). The detailed steps of

the BRMRS strategy are depicted in Sub-algorithm 3. It starts with step 1 to first calculate the D2D rates for each candidate relay lying inside the DA. Then, the result is stored in the relay rate matrix U_{rs}. After that, the best relay is determined based on the maximum achieved rate. In step 2, the harvested and residual energies of the TWR D2D Links are determined.

Sub-Algorithm 3 Rate Maximization RS Sub-Algorithm (BRMRS)

Input: P_{max}, $P^{opt}_{s1,w}$, $P^{opt}_{s2,w}$, $P^{opt}_{rl,w}$,η^{RF}, $\rho^{opt}_{rl,w}$, E_{max}, $\boldsymbol{G}$.
Output: $\mathcal{R}_\psi$, Relays rate matrix U_{rs}, $E^{h}_{rl,w}$, $E^{Res}_{rl,w}$.

Initialization: $l = 1$
Step 1: Determine $\mathcal{R}_\psi$
for each relay l inside the DA **do**
  Calculate R^{D2D}_{sum} achieved by R_l.
  $U_{rs} \leftarrow (l,R^{D2D}_{sum})$.
end for
for each relay l inside the DA **do**
  Calculate average residual energy by all relays E^{res}_{avg}.
end for
if $E^{Res}_{rl,w} \geq E^{res}_{avg}$ **then**
  Find R_l in U_R that achieves maximum TWR D2D link rate following (30a).
  $\mathcal{R}_\psi \leftarrow R_l$
end if
Step 2: Determine harvested and residual energies of the TWR D2D Links
while $l \leq L$ inside DA **do**
  if l equals to S **then**
    Calculate $E^{h}_{rl,w}$ and $E^{Res}_{rl,w}$ following (13) and (14), respectively, for $\beta^{(n)}_{mrl,w} = 1$.
  else
    Calculate $E^{h}_{rl,w}$ and $E^{Res}_{rl,w}$ following (13) and (14), respectively, for $\beta^{(n)}_{mrl,w} = 0$.
  end if
  $l = l + 1$
end while

C. THE JPARS-EH ALGORITHM

Here, we combine the two aforementioned sub-algorithms, EHPA and BRMRS, into the JPARS-EH algorithm that is capable of maximizing the TWR D2D link data rate. The details of the proposed algorithm are shown in Algorithm 4. This algorithm assumes that the UL resources are already allocated by the BS assuming the channel gain matrix $\boldsymbol{G}$. The algorithm starts with solving the PA sub-problem in Step 1. In this step, the transmission power of the two D2D terminals P_{s_1} and P_{s_2}, the relay transmit power P_{r_l}, and the PS factor ρ_{r_l} are optimally determined relying on the PSO algorithm. This is achieved following the QoS constraints and the EH causality constraints of the relays as well as the maximum practical transmit power. During Step 2, the best relay that lies in the DA with residual energy above the average is selected. This is performed taking into account the residual energy condition relying on constraint (14) with the overflow constraint represented by (21h).

On one side, the PA of the conventional users is performed in a centralized way by the BS. On the other side, the TWR D2D links take are responsible for their PA strategy relying on the PSO algorithm distributively. This can be done relying on the relays' remaining energy following the EH ability of the TWR links. Besides, the JPARS-EH algorithm provides a feasible switching between the partially network-aided and fully network-aided peer discovery mechanisms [68], [69].

1) Big O Notation Analysis: Here, we aim at investigating the computational complexity of the proposed algorithm concerning the big O notation. It is worth mentioning that we consider M TWR D2D links, where the JPARS-EH algorithm performs the PA and RS processes for each link resulting in two major sub-algorithms namely EHPA and BRMRS, respectively. The EHPA sub-algorithm aims to utilize the PSO algorithm to allocate the optimal transmission power of the M links. It is well known that the number of PSO solutions $\mathcal{N}$, the maximum number of iterations T_{max},, and the dimension of each solution Dim represent the computational complexity of any algorithm that relies on the PSO [67]. Accordingly, the computational complexity of the EHPA sub-algorithm can be defined as $O|M * T_{max}(Dim * \mathcal{N} + \mathcal{N}^2)|$ for M links, which can be rewritten as $O|M * T_{max} * \mathcal{N}^2)|$ since $Dim < \mathcal{N}$.

Sub-algorithm 3 defines the BRMRS strategy that selects the optimal relay that maximizes the TWR D2D link rate among the candidates, which lie in the DA. In step 1, it is required to calculate the data rate for every relay l inside the DA with complexity $O|L_{DA}|$, while the complexity of $O|L^2_{DA}|$ is needed to perform quick-sorting for these rates. Thus, the big O notation for step 1 is $O|L^2_{DA}|$. The harvested and residual energy is calculated in step 2 resulting in a complexity of $O|L_{DA}|$. Accordingly, for M links, the overall computation complexity of Sub-algorithm 3 is $O|M * L^2_{DA}|$. In a nutshell, the worst-case computational complexity of the JPARS-EH algorithm is $O|M * (T_{max} * \mathcal{N}^2 + L^2_{DA})|$, while its best-case big O notation complexity is $O|M * (T_{max} * \mathcal{N}\log(\mathcal{N}) + L_{DA}\log(L_{DA}))|$.

V. NUMERICAL ANALYSIS

In this section, the performance of the JPARS-EH algorithm is investigated concerning various parameters. Besides, it is compared to one of the most recent EH-aided OWR algorithms namely RPRS-EH in addition to the UL-*max* algorithm. The comparison shows the impact of the TWR technology on the EH D2D communication performance underlaying conventional cellular networks when compared to that of the OWR. In Table 2, the main simulation parameters used for our results are shown unless otherwise stated. It is important to note that all the next results show the performance of one TWR D2D link m sharing the resources of one CU k at time slot w. Furthermore, it is assumed that there is no direct link between S_1 and S_2 due to the high channel attenuation between them. Also, the EH data is acquired from the solar EH real-life data set available at the NREL. The data

Algorithm 4 JPARS-EH

Input: P_{max}, γ_{min}, E_{max}, η^{RF}, $\boldsymbol{G}$.
Output: U_{rs}, $\mathcal{R}_\psi$, $E^{h}_{r_l,w}$, $E^{Res}_{r_l,w}$, $\rho^{opt}_{r_l,w}$, $P^{opt}_{s_1,w}$, $P^{opt}_{s_2,w}$, $P^{opt}_{r_l,w}$.

1: **Initialization:** $P_{c,w} = P_{max}$, UL resource sharing is assumed to be performed.
2: **Step 1: Power allocation sub-algorithm EHPA**
3: Select the PSO parameters (i.e., P_{s_1}, P_{s_2}, P_{r_l}, and ρ_{r_l}).
4: Determine the lower and upper boundaries of the selected parameters from (5), (6), (3), (11), (12), (8), and (21c) considering the maximum power limit in (21e) and the causality constraint in (21g).
5: Determine the optimal PA allocation parameters relying on Step 2 in Sub-algorithm 2.
6: **Step 2: Relay selection sub-algorithm (BRMRS)**
7: **for** each relay l that lies in the DA with residual energy above the average **do**
8: Select R_l that maximizes the TWR D2D link rate and then assign it as $\mathcal{R}_\psi \leftarrow R_l$.
9: Calculate $E^{h}_{r_l,w}$ according to (13).
10: Calculate $E^{Res}_{r_l,w}$ according to (14) taking into account the overflow constraint in (21h).
11: **end for**

TABLE 2. Simulation parameters.

Parameter	Value
Cell radius	500 m
Number of cellular users (K)	10
Number of D2D links (M)	5
Number of relays (L)	100
Sub-channel max. power (P_{max})	24 dBm
Minimum SINR value (γ_{min})	5 dB
Path loss exponent (ν)	3.5
Distance between S_1 and S_2 ($\mathcal{D}$)	100 m
Max. EH amount of relays (E_{max})	100 mJ
Time slot duration(T_c)	1 s
RF conversion efficiency(η^{RF})	0.7
Noise power (σ^2)	-174 dBm/Hz
Number of Iterations	20
Number of solutions ($\mathcal{N}$)	20
Initial inertia weight	0.5
The acceleration coefficients	1.4

is captured in Los Angeles city during June. Furthermore, each RN is supported with a small solar cell of 90mm x 25mm (LxW) dimensions.

The impact of varying the distance between the TWR D2D link m and CL k (i.e., D_{mk}) on the TWR D2D link rate of the JPARS-EH algorithm is investigated in Figure 4. Besides, the performance of the proposed algorithm is compared to the RPRS-EH and UL-*max* algorithms. It is clear from the figure that the more the D_{mk}, the less the interference imposed from CL k on D2D link m, and the more the D2D link rate. Also, the results depict the D2D link rate advantage of the JPARS-EH algorithm over the two other algorithms. This is because of the use of the TWR model in our proposal instead of using the OWR model. In Figure 5, the impact of changing P_{max} on the TWR D2D link rate of the JPARS-EH, RPRS-EH, and UL-*max* algorithms is shown. When P_{max} increases, the chance to compensate for the power loss due to the traveling

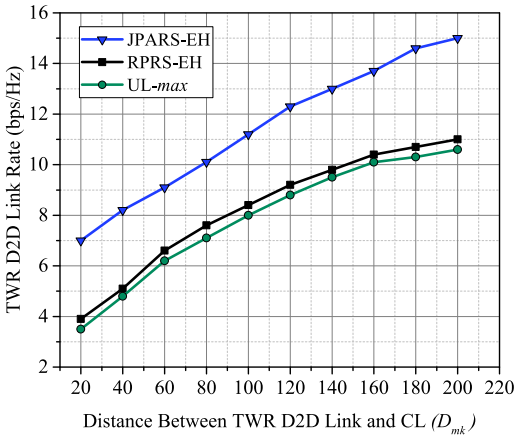

FIGURE 4. The effect of varying D_{mk} on the TWR D2D link rate.

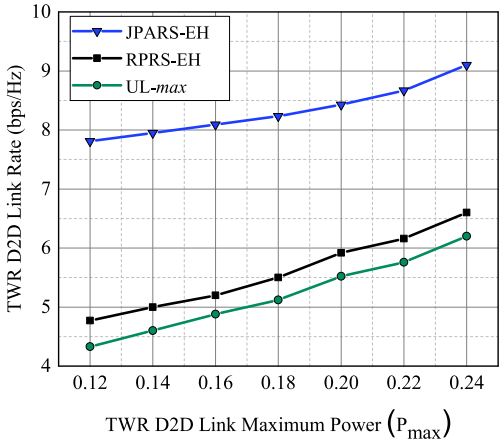

FIGURE 5. The impact of varying the maximum D2D link allowed transmission power on the TWR D2D link rate.

distance increases. Hence, the TWR D2D link rate increases with increasing P_{max} for the three curves keeping better performance for the JPARS-EH algorithm.

The relation between the summation of S_1 and S_2 transmission powers (i.e., P_{s_1} and P_{s_2}) and distance variation between the two terminals for the proposed algorithm is depicted in Figure 6. Clearly, the more the distance between the two terminals, the more the transmission power of S_1 and S_2 to compensate for the power degradation due to distance increase. Thus, the TWR D2D link rate maximization is guaranteed considering the maximum power limit and energy constraints. Here, the RPRS-EH and UL-*max* are not considered for comparison since they are OWR models and their terminals S_1 and S_2 can not transmit simultaneously.

Figure 7 shows the relation between the RF EH amount of $\mathcal{R}_\psi$ and the distance between the two terminals $\mathcal{D}$ for the JPARS-EH and RPRS-EH algorithms. Since the UL-*max* does not support the EH capability, it is not considered for comparison in this figure. The figure illustrates that the amount of energy harvested by $\mathcal{R}_\psi$ decreases upon increasing the distance between S_1 and S_2. This is because the received power at $\mathcal{R}_\psi$ attenuates proportionally with the traveled distance. However, the proposed algorithm shows

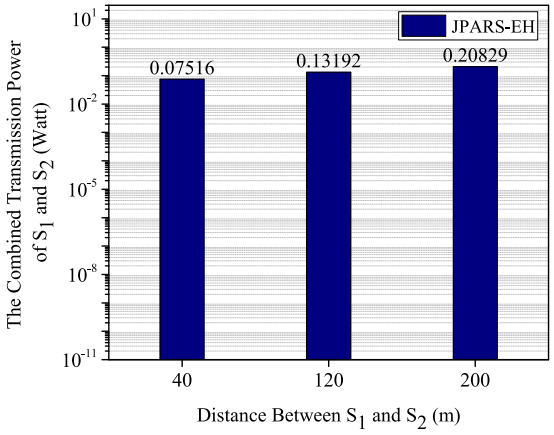

FIGURE 6. The relation between the combined transmission power of both S_1 and S_2 and the distance variation between them.

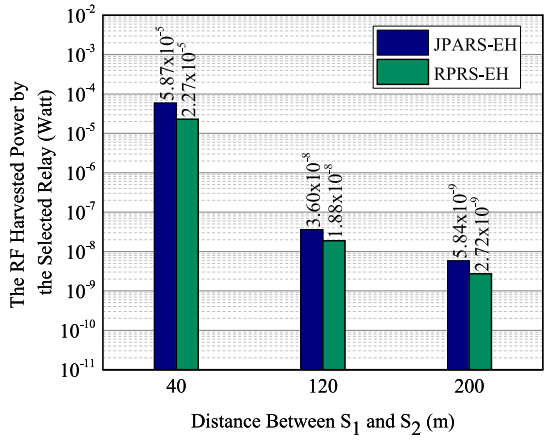

FIGURE 7. The RF power harvested by $\mathcal{R}_\psi$ versus the distance between S_1 and S_2.

more EH amount by R_ψ when compared to the RPRS-EH. This is due to the EH advantage of the TWR paradigm over that of the OWR model. Thus, the TWR D2D communication achieves better EE.

Figure 8 illustrates the impact of the number of the EHRs on the TWR D2D link rate for the JPARS-EH, RPRS-EH, and UL-*max* at $\mathcal{D} = 100$. Indeed, increasing the number of relays gives more chances for selecting an EHR with better channel and position conditions that achieve a higher TWR D2D link rate. Thus, the D2D link rate increases when increasing L as depicted in Figure 8. Again, our TWR proposal with its DA mechanism gives better performance when compared to the two others.

In Figure 9, the JPARS-EH algorithm is compared to the RPRS-EH and UL-*max* algorithms investigating the impact of varying the distance between S_1 and S_2 on the D2D link rate. The results depict that the D2D link rate decays with the distance increase for the three algorithms. Indeed, the proposed algorithm shows better D2D link rate than the RPRS-EH and UL-*max* algorithms as it exploits the TWR feature, which performs data transmission in two phases instead

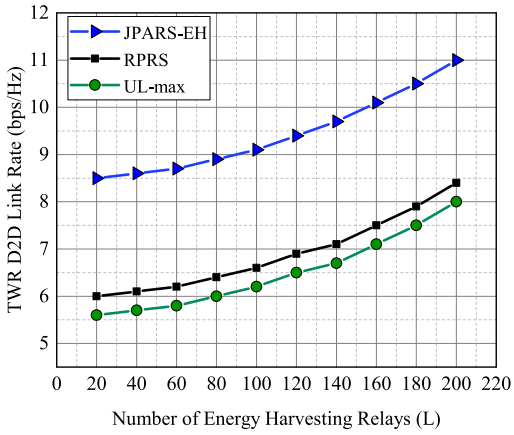

FIGURE 8. The impact of varying the number of EHRs on the D2D link rate.

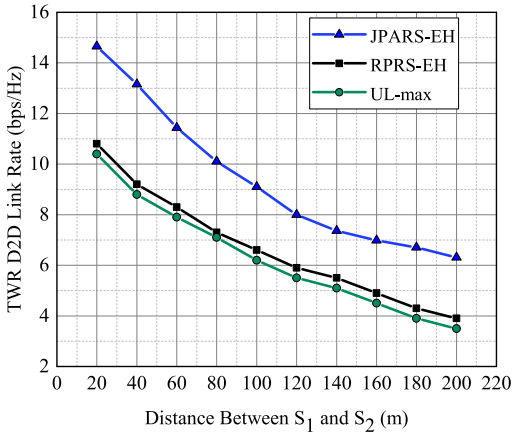

FIGURE 9. The impact of varying the distance between S_1 and S_2 on the D2D link rate.

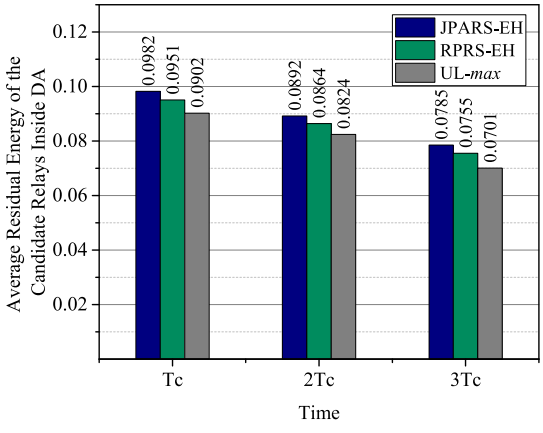

FIGURE 10. Average residual energy of candidate relays inside the DA.

of four like the OWR technology. This comes with better EH for the relays capabilities as shown in Figure 7.

Figure 10 depicts the impact of the BRMRS strategy on the average residual energy of the candidate relays inside the DA for the JPARS-EH algorithm. The results show a comparison between the JPARS-EH, RPRS-EH, and UL-*max* algorithms for different transmission times and $\mathcal{D}$ =100 m. In the case of the JPARS-EH algorithm, it is shown that the average

residual energy of the candidate relays is always higher than that of the two other algorithms. In the BRMRS strategy of the JPARS-EH, only relays with residual energy above the average and lie inside the DA are considered as candidates. This balances the energy consumption among the candidates and increases their average residual energy. Thus, the overall D2D communication EE is improved. Also, the JPARS-EH algorithm gives more significance in terms of the average residual energy due to the TWR EH capability when compared RPRS-EH and UL-*max* algorithm (see Figure 7). It is worth mentioning that the RPRS-EH has an OWR EH capability, while the UL-*max* has no EH capability. Therefore, this gives more advantages to our proposal.

VI. CONCLUSION

In this paper, we study the problem of joint PA and RS for the EH TWR D2D communication links that share the UL spectrum of the cellular network. In addition, the participated relays are considered hybrid RF/RE-based EHRs. To maximize the TWR D2D links rate, the JPARS-EH algorithm is developed to jointly optimize the transmission power of all users and the PS factor of relays based on the well-known meta-heuristic algorithm PSO. Besides, the best relay is selected based on the DA mechanism taking the balanced energy consumption of the relays into account. The numerical results show the consistent behavior of the JPARS-EH algorithm concerning different simulation parameters. Furthermore, the proposed algorithm is compared to two of the most recent EH OWR D2D communication algorithms called the RPRS-EH and UL-*max*. It is clearly shown in the results that the JPARS-EH algorithm outperforms the RPRS-EH algorithm in terms of the D2D link rate and EE. As a part of the future work, it is expected to integrate the IRS and UAV technologies with our model so the D2D performance can be boosted. Last but not least, future work should take into account the imperfect CSI assuming the channel gain variation at each time slot.

REFERENCES

[1] A. Gupta and R. K. Jha, "A survey of 5G network: Architecture and emerging technologies," *IEEE Access*, vol. 3, pp. 1206–1232, 2015, doi: 10.1109/ACCESS.2015.2461602.

[2] G. Zhang, K. Yang, and H.-H. Chen, "Socially aware cluster formation and radio resource allocation in D2D networks," *IEEE Wireless Commun.*, vol. 23, no. 4, pp. 68–73, Aug. 2016, doi: 10.1109/MWC.2016.7553028.

[3] O. Hashad, M. M. Fouda, A. S. T. Eldien, E. M. Mohamed, and B. M. Elhalawany, "Resources allocation in underlay device-to-device communications networks: A reduced-constraints approach," *IEEE Access*, vol. 8, pp. 228891–228904, 2020, doi: 10.1109/ACCESS.2020.3046417.

[4] O. Hashad, B. M. ElHalawany, M. M. Fouda, and A. S. T. Eldien, "Joint resources allocation of device-to-device communications underlaying cellular networks," in *Proc. 7th Int. Jpn.-Africa Conf. Electron., Commun., Comput., (JAC-ECC)*, Dec. 2019, pp. 32–36, doi: 10.1109/JAC-ECC48896.2019.9051283.

[5] J. Zhang, Y. Zhang, L. Xiang, Y. Sun, D. W. K. Ng, and M. Jo, "Robust energy-efficient transmission for wireless-powered D2D communication networks," *IEEE Trans. Veh. Technol.*, vol. 70, no. 8, pp. 7951–7965, Aug. 2021, doi: 10.1109/TVT.2021.3095626.

[6] A. He, L. Wang, Y. Chen, K.-K. Wong, and M. Elkashlan, "Spectral and energy efficiency of uplink D2D underlaid massive MIMO cellular networks," *IEEE Trans. Commun.*, vol. 65, no. 9, pp. 3780–3793, Sep. 2017, doi: 10.1109/TCOMM.2017.2712708.

[7] S. K. Rashed, R. Asvadi, S. Rajabi, S. A. Ghorashi, and M. G. Martini, "Power allocation for D2D communications using max-min message-passing algorithm," *IEEE Trans. Veh. Technol.*, vol. 69, no. 8, pp. 8443–8458, Aug. 2020, doi: 10.1109/TVT.2020.2995534.

[8] Y. Dai, M. Sheng, J. Liu, N. Cheng, X. Shen, and Q. Yang, "Joint mode selection and resource allocation for D2D-enabled NOMA cellular networks," *IEEE Trans. Veh. Technol.*, vol. 68, no. 7, pp. 6721–6733, Jul. 2019, doi: 10.1109/TVT.2019.2916395.

[9] D. C. Nguyen, M. Ding, P. N. Pathirana, A. Seneviratne, J. Li, D. Niyato, O. Dobre, and H. V. Poor, "6G Internet of Things: A comprehensive survey," *IEEE Internet Things J.*, vol. 9, no. 1, pp. 359–383, Jan. 2022, doi: 10.1109/JIOT.2021.3103320.

[10] R. Raj, K. Jindal, and A. Dixit, "Fairness enhancement of non-orthogonal multiple access in VLC-based IoT networks for intravehicular applications," *IEEE Trans. Veh. Technol.*, vol. 71, no. 7, pp. 7414–7427, Jul. 2022, doi: 10.1109/TVT.2022.3167091.

[11] L. Lyu, C. Chen, N. Cheng, S. Zhu, X. Guan, and X. Shen, "NOMA-assisted on-demand transmissions for monitoring applications in industrial IoT networks," *IEEE Trans. Veh. Technol.*, vol. 69, no. 10, pp. 12264–12276, Oct. 2020, doi: 10.1109/TVT.2020.3020298.

[12] M. S. Abdalzaher, S. S. R. Moustafa, H. E. A. Hafiez, and W. F. Ahmed, "An optimized learning model augment analyst decisions for seismic source discrimination," *IEEE Trans. Geosci. Remote Sens.*, vol. 60, pp. 1–12, 2022.

[13] O. Hamdy, H. Gaber, M. S. Abdalzaher, and M. Elhadidy, "Identifying exposure of urban area to certain seismic hazard using machine learning and GIS: A case study of greater Cairo," *Sustainability*, vol. 14, no. 17, Aug. 2022, Art. no. 10722.

[14] S. S. R. Moustafa, M. S. Abdalzaher, M. Naeem, and M. M. Fouda, "Seismic hazard and site suitability evaluation based on multicriteria decision analysis," *IEEE Access*, vol. 10, pp. 69511–69530, 2022.

[15] S. S. R. Moustafa, M. S. Abdalzaher, F. Khan, M. Metwaly, E. A. Elawadi, and N. S. Al-Arifi, "A quantitative site-specific classification approach based on affinity propagation clustering," *IEEE Access*, vol. 9, pp. 155297–155313, 2021.

[16] M. S. Abdalzaher, S. S. R. Moustafa, M. Abd-Elnaby, and M. Elwekeil, "Comparative performance assessments of machine-learning methods for artificial seismic sources discrimination," *IEEE Access*, vol. 9, pp. 65524–65535, 2021.

[17] S. S. R. Moustafa, M. S. Abdalzaher, M. H. Yassien, T. Wang, M. Elwekeil, and H. E. A. Hafiez, "Development of an optimized regression model to predict blast-driven ground vibrations," *IEEE Access*, vol. 9, pp. 31826–31841, 2021.

[18] M. Elhadidy, M. S. Abdalzaher, and H. Gaber, "Up-to-date PSHA along the Gulf of aqaba-dead sea transform fault," *Soil Dyn. Earthq. Eng.*, vol. 148, Sep. 2021, Art. no. 106835.

[19] M. S. Abdalzaher, M. El-Hadidy, H. Gaber, and A. Badawy, "Seismic hazard maps of Egypt based on spatially smoothed seismicity model and recent seismotectonic models," *J. Afr. Earth Sci.*, vol. 170, Oct. 2020, Art. no. 103894.

[20] S. W. H. Shah, A. N. Mian, S. Mumtaz, A. Al-Dulaimi, I. Chih-Lin, and J. Crowcroft, "Statistical QoS analysis of reconfigurable intelligent surface-assisted D2D communication," *IEEE Trans. Veh. Technol.*, vol. 71, no. 7, pp. 7343–7358, Jul. 2022.

[21] M. S. Abdalzaher, L. Samy, and O. Muta, "Non-zero-sum game-based trust model to enhance wireless sensor networks security for IoT applications," *IET Wireless Sensor Syst.*, vol. 9, no. 4, pp. 218–226, Aug. 2019.

[22] M. S. Abdalzaher and O. Muta, "Employing game theory and TDMA protocol to enhance security and manage power consumption in WSNs-based cognitive radio," *IEEE Access*, vol. 7, pp. 132923–132936, 2019.

[23] M. S. Abdalzaher and O. Muta, "A game-theoretic approach for enhancing security and data trustworthiness in IoT applications," *IEEE Internet Things J.*, vol. 7, no. 11, pp. 11250–11261, Nov. 2020.

[24] M. S. Abdalzaher and H. A. Elsayed, "Employing data communication networks for managing safer evacuation during earthquake disaster," *Simul. Model. Pract. Theory*, vol. 94, pp. 379–394, Jul. 2019.

[25] M. S. Abdalzaher, M. S. Soliman, S. M. El-Hady, A. Benslimane, and M. Elwekeil, "A deep learning model for earthquake parameters observation in IoT system-based earthquake early warning," *IEEE Internet Things J.*, vol. 9, no. 11, pp. 8412–8424, Jun. 2022.

[26] M. S. Abdalzaher, M. Elwekeil, T. Wang, and S. Zhang, "A deep autoencoder trust model for mitigating jamming attack in IoT assisted by cognitive radio," *IEEE Syst. J.*, vol. 16, no. 3, pp. 3635–3645, Sep. 2022.

[27] M. S. Abdalzaher, K. Seddik, and O. Muta, "Using Stackelberg game to enhance cognitive radio sensor networks security," *IET Commun.*, vol. 11, no. 9, pp. 1503–1511, Jun. 2017.
[28] M. Abdalzaher, K. Seddik, M. Elsabrouty, O. Muta, H. Furukawa, and A. Abdel-Rahman, "Game theory meets wireless sensor networks security requirements and threats mitigation: A survey," *Sensors*, vol. 16, no. 7, p. 1003, Jun. 2016.
[29] M. S. Abdalzaher, K. Seddik, O. Muta, and A. Abdelrahman, "Using Stackelberg game to enhance node protection in WSNs," in *Proc. 13th IEEE Annu. Consum. Commun. Netw. Conf. (CCNC)*, Jan. 2016, pp. 853–856.
[30] M. Elwekeil, M. S. Abdalzaher, and K. Seddik, "Prolonging smart grid network lifetime through optimising number of sensor nodes and packet length," *IET Commun.*, vol. 13, no. 16, pp. 2478–2484, Oct. 2019.
[31] M. S. Abdalzaher, K. Seddik, and O. Muta, "Using repeated game for maximizing high priority data trustworthiness in wireless sensor networks," in *Proc. IEEE Symp. Comput. Commun. (ISCC)*, Jul. 2017, pp. 552–557.
[32] M. S. Abdalzaher, K. Seddik, and O. Muta, "An effective Stackelberg game for high-assurance of data trustworthiness in WSNs," in *Proc. IEEE Symp. Comput. Commun. (ISCC)*, Jul. 2017, pp. 1257–1262.
[33] Z. Zhao, Z. Ding, M. Peng, and Y. Li, "A full-cooperative diversity beamformingscheme in two-way amplify-and-forward relay systems," *Digit. Commun. Netw.*, vol. 1, no. 1, pp. 57–67, Feb. 2015, doi: 10.1016/j.dcan.2015.02.005.
[34] H. Gao, S. Zhang, Y. Su, and M. Diao, "Joint resource allocation and power control algorithm for cooperative D2D heterogeneous networks," *IEEE Access*, vol. 7, pp. 20632–20643, 2019, doi: 10.1109/ACCESS.2019.2895975.
[35] M. Rahman, Y. Lee, and I. Koo, "Energy-efficient power allocation and relay selection schemes for relay-assisted D2D communications in 5G wireless networks," *Sensors*, vol. 18, no. 9, p. 2865, Aug. 2018.
[36] S. Dang, G. Chen, and J. P. Coon, "Multicarrier relay selection for full-duplex relay-assisted OFDM D2D systems," *IEEE Trans. Veh. Technol.*, vol. 67, no. 8, pp. 7204–7218, Aug. 2018, doi: 10.1109/TVT.2018.2829401.
[37] E. M. Mohamed, H. S. Khallaf, M. Uysal, B. M. ElHalawany, and M. M. Fouda, "Wi-Fi assisted two-hop relay probing in WiGig device to device networks," in *Proc. IEEE Int. Conf. Commun.*, Jun. 2021, pp. 1–6, doi: 10.1109/ICC42927.2021.9500965.
[38] E. M. Mohamed, S. Hashima, K. Hatano, M. M. Fouda, and Z. M. Fadlullah, "Sleeping contextual/non-contextual Thompson sampling MAB for mmWave D2D two-hop relay probing," *IEEE Trans. Veh. Technol.*, vol. 70, no. 11, pp. 12101–12112, Nov. 2021, doi: 10.1109/TVT.2021.3116223.
[39] J. Cao, X. Song, Z. Xie, S. Li, and F. Si, "Social-aware relay selection and energy-efficient resource allocation for relay-aided D2D communication," *Phys. Commun.*, vol. 52, Jun. 2022, Art. no. 101665, doi: 10.1016/j.phycom.2022.101665.
[40] Y. Cai, C. Ke, Y. Ni, J. Zhang, and H. Zhu, "Power allocation for NOMA in D2D relay communications," *China Commun.*, vol. 18, no. 1, pp. 61–69, Jan. 2021, doi: 10.23919/JCC.2021.01.006.
[41] A. Alsharoa, H. Ghazzai, A. E. Kamal, and A. Kadri, "Optimization of a power splitting protocol for two-way multiple energy harvesting relay system," *IEEE Trans. Green Commun. Netw.*, vol. 1, no. 4, pp. 444–457, Dec. 2017, doi: 10.1109/TGCN.2017.2724438.
[42] N. T. Tung, P. M. Nam, and P. T. Tin, "Performance evaluation of a two-way relay network with energy harvesting and hardware noises," *Digit. Commun. Netw.*, vol. 7, no. 1, pp. 45–54, Feb. 2021, doi: 10.1016/j.dcan.2020.04.003.
[43] Y. Cai, Y. Ni, J. Zhang, S. Zhao, and H. Zhu, "Energy efficiency and spectrum efficiency in underlay device-to-device communications enabled cellular networks," *China Commun.*, vol. 16, no. 4, pp. 16–34, 2019, doi: 10.12676/j.cc.2019.04.002.
[44] J. Qian and C. Masouros, "On the effects of channel aging in D2D two-way relaying with space-constrained massive MIMO," in *Proc. IEEE Globecom Workshops (GC Wkshps*, Dec. 2020, pp. 1–6, doi: 10.1109/GCWkshps50303.2020.9367524.
[45] Y. Pei and Y.-C. Liang, "Resource allocation for device-to-device communications overlaying two-way cellular networks," *IEEE Trans. Wireless Commun.*, vol. 12, no. 7, pp. 3611–3621, Jul. 2013, doi: 10.1109/TWC.2013.061713.121956.
[46] J. Huang and H. Gharavi, "Performance analysis of relay-based two-way D2D communications with network coding," *IEEE Trans. Veh. Technol.*, vol. 67, no. 7, pp. 6642–6646, Jul. 2018, doi: 10.1109/TVT.2018.2797123.
[47] Y. Xu and B. Liu, "Disaster-recovery communications utilizing SWIPT-based D2D relay network," in *Proc. IEEE 5th Int. Conf. Comput. Commun. (ICCC)*, Dec. 2019, pp. 1041–1046, doi: 10.1109/ICCC47050.2019.9064404.
[48] H.-P. Dang, M.-S. Van Nguyen, D.-T. Do, H.-L. Pham, B. Selim, and G. Kaddoum, "Joint relay selection, full-duplex and device-to-device transmission in wireless powered NOMA networks," *IEEE Access*, vol. 8, pp. 82442–82460, 2020, doi: 10.1109/ACCESS.2020.2991847.
[49] M. M. Salim, D. Wang, Y. Liu, H. A. El Atty Elsayed, and M. A. Elaziz, "Optimal resource and power allocation with relay selection for RF/RE energy harvesting relay-aided D2D communication," *IEEE Access*, vol. 7, pp. 89670–89686, 2019, doi: 10.1109/ACCESS.2019.2924026.
[50] S. Kurma, P. K. Sharma, K. Singh, S. Mumtaz, and C.-P. Li, "URLLC based cooperative industrial IoT networks with non-linear energy harvesting," *IEEE Trans. Ind. Informat.*, early access, Apr. 12, 2022, doi: 10.1109/TII.2022.3166808.
[51] J. Huang, C.-C. Xing, and C. Wang, "Simultaneous wireless information and power transfer: Technologies, applications, and research challenges," *IEEE Commun. Mag.*, vol. 55, no. 11, pp. 26–32, Nov. 2017, doi: 10.1109/MCOM.2017.1600806.
[52] N. Kumar Jadav, R. Gupta, and S. Tanwar, "A survey on energy-efficient resource allocation schemes in device-to-device communication," *Int. J. Commun. Syst.*, vol. 35, no. 8, May 2022, Art. no. e5112, doi: 10.1002/dac.5112.
[53] E. Ghamry, E. K. Mohamed, M. S. Abdalzaher, M. Elwekeil, D. Marchetti, A. D. Santis, M. Hegy, A. Yoshikawa, and A. Fathy, "Integrating pre-earthquake signatures from different precursor tools," *IEEE Access*, vol. 9, pp. 33268–33283, 2021.
[54] V. Kaur and S. Thangjam, "RF energy harvesting based D2D communication in downlink cellular network with repulsion point process modeling," in *Proc. 9th Int. Conf. Contemp. Comput. (IC)*, Aug. 2016, pp. 1–5, doi: 10.1109/IC3.2016.7880241.
[55] I. Budhiraja, N. Kumar, S. Tyagi, S. Tanwar, and M. Guizani, "SWIPT-enabled D2D communication underlaying NOMA-based cellular networks in imperfect CSI," *IEEE Trans. Veh. Technol.*, vol. 70, no. 1, pp. 692–699, Jan. 2021, doi: 10.1109/TVT.2021.3049185.
[56] L. Wei, R. Q. Hu, Y. Qian, and G. Wu, "Energy efficiency and spectrum efficiency of multihop device-to-device communications underlaying cellular networks," *IEEE Trans. Veh. Technol.*, vol. 65, no. 1, pp. 367–380, Jan. 2016.
[57] Q. Li and P. Ren, "Collaborative D2D communication in relay networks with energy harvesting," *China Commun.*, vol. 19, no. 9, pp. 162–170, Sep. 2022, doi: 10.23919/JCC.2022.00.007.
[58] G. Si, Z. Dou, Y. Lin, L. Qi, and M. Wang, "Relay selection and secure connectivity analysis in energy harvesting multi-hop D2D networks," *IEEE Commun. Lett.*, vol. 26, no. 6, pp. 1245–1248, Jun. 2022, doi: 10.1109/LCOMM.2021.3135469.
[59] L. Han, R. Zhou, Y. Li, B. Zhang, and X. Zhang, "Power control for two-way AF relay assisted D2D communications underlaying cellular networks," *IEEE Access*, vol. 8, pp. 151968–151975, 2020, doi: 10.1109/ACCESS.2020.3017799.
[60] S. Zhang and Y. Peng, "D2D communication relay selection algorithm based on game theory," *Proc. Comput. Sci.*, vol. 166, pp. 563–569, Jan. 2020, doi: 10.1016/j.procs.2020.02.020.
[61] J. Sun, Z. Zhang, C. Xing, and H. Xiao, "Uplink resource allocation for relay-aided device-to-device communication," *IEEE Trans. Intell. Transp. Syst.*, vol. 19, no. 12, pp. 3883–3892, Dec. 2018, doi: 10.1109/TITS.2017.2788562.
[62] X. Jin, H. Jiang, J. Hu, Y. Yuan, C. Zhao, and J. Shi, "Maximum data rate power allocation for MIMO spatial multiplexing systems with imperfect CSI," in *Proc. VTC Spring IEEE 69th Veh. Technol. Conf.*, Apr. 2009, pp. 1–5.
[63] T. M. Hoang, N. L. Van, B. C. Nguyen, and L. T. Dung, "On the performance of energy harvesting non-orthogonal multiple access relaying system with imperfect channel state information over Rayleigh fading channels," *Sensors*, vol. 19, no. 15, p. 3327, Jul. 2019.
[64] M. M. Salim, D. Wang, H. A. El A. Elsayed, Y. Liu, and M. A. Elaziz, "Joint optimization of energy-harvesting-powered two-way relaying D2D communication for IoT: A rate–energy efficiency tradeoff," *IEEE Internet Things J.*, vol. 7, no. 12, pp. 11735–11752, Dec. 2020.
[65] C. Peng, F. Li, and H. Liu, "Optimal power splitting in two-way decode-and-forward relay networks," *IEEE Commun. Lett.*, vol. 21, no. 9, pp. 2009–2012, Sep. 2017, doi: 10.1109/LCOMM.2017.2671363.

[66] *NREL: Measurement and Instrumentation Data Center*. Accessed: Apr. 2022. [Online]. Available: https://www.nrel.gov/midc/
[67] J. Kennedy and R. Eberhart, "Particle swarm optimization," in *Proc. IEEE ICNN*, vol. 4, Nov./Dec. 1995, pp. 1942–1948, doi: 10.1109/ICNN.1995.488968.
[68] Z. Kaleem, N. N. Qadri, T. Q. Duong, and G. K. Karagiannidis, "Energy-efficient device discovery in D2D cellular networks for public safety scenario," *IEEE Syst. J.*, vol. 13, no. 3, pp. 2716–2719, Sep. 2019.
[69] O. Hayat, R. Ngah, S. Z. M. Hashim, M. H. Dahri, R. F. Malik, and Y. Rahayu, "Device discovery in D2D communication: A survey," *IEEE Access*, vol. 7, pp. 131114–131134, 2019, doi: 10.1109/ACCESS.2019.2941138.

MAHMOUD M. SALIM received the B.S. degree in computer engineering from October 6 University, Egypt, in 2008, the M.S. degree in wireless sensor networks (WSNs) from Ain Shams University, Egypt, in 2014, and the Ph.D. degree from the School of EIC, Huazhong University of Science and Technology (HUST), Wuhan, China. He is currently an Assistant Professor at the Department of Communications Engineering, October 6 University. He has published articles in top-tier journals, such as IEEE Access and IEEE Internet of Things Journal. Also, he has received a Graduation Project Fund granted by the Information Technology Industry Development Agency (ITIDA), Egypt. His research interests include computer and mobile networking, especially radio resource allocation, power allocation, and energy efficiency of device-to-device (D2D) communication in cellular networks in addition to medium access control (MAC) and routing algorithms of wireless sensor networks (WSNs). Recently, he is interested in the IoT intelligent applications, such as V2X and relying on machine learning.

HUSSEIN A. ELSAYED (Member, IEEE) received the B.Sc. and M.Sc. degrees from the Electronics and Communications Engineering Department, Faculty of Engineering, Ain Shams University, Cairo, Egypt, in 1991 and 1995, respectively, and the Ph.D. degree from the Electrical Engineering Department, City University of New York, New York, NY, USA, in 2003. He is currently a Professor with the Electronics and Communications Engineering Department, Faculty of Engineering, Ain Shams University. Since graduated, he served in different positions and built both practical and theoretical skills in the area of telecommunication networks. He supervised and joined several telecommunication graduation, research, and laboratory/operational projects, including service provider Network Operation Center (NOC). His research interests include ad hoc networks, cognitive radio networks (CRN), wireless sensor networks (WSN), medium access control (MAC), routing protocols, software-defined networks (SDN), device-to-device communication (D2D), and mobile systems, where he has a long list of publications.

MOHAMED ABD ELAZIZ received the B.S. and M.S. degrees in computer science and the Ph.D. degree in mathematics and computer science from Zagazig University, Egypt, in 2008, 2011, and 2014, respectively. From 2008 to 2011, he was an Assistant Lecturer with the Department of Computer Science. Since 2014, he has been a Lecturer with the Mathematical Department, Zagazig University. He is the author of more than 50 articles. His research interests include machine learning, signal processing, image processing, and metaheuristic techniques.

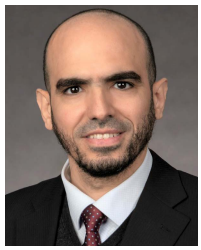

MOSTAFA M. FOUDA (Senior Member, IEEE) received the B.S.E.E. (as the valedictorian) and M.S.E.E. degrees from Benha University, Egypt, and the Ph.D. degree in information sciences from Tohoku University, Japan. He was an Assistant Professor at Tohoku University and a Postdoctoral Research Associate at Tennessee Technological University, Cookeville, TN, USA. He is currently an Assistant Professor with the Department of Electrical and Computer Engineering, Idaho State University, Pocatello, ID, USA. He also holds the position of a Full Professor at Benha University. He has (co)authored more than 120 technical publications. His current research interests include cybersecurity, communication networks, signal processing, wireless mobile communications, smart healthcare, smart grids, AI, and the IoT. He has received several research grants, including NSF-JUNO3. He has guest-edited a number of special issues covering various emerging topics in communications, networking, and health analytics. He is also serving on the Editorial Board of IEEE Transactions on Vehicular Technology (TVT) and IEEE Access.

MOHAMED S. ABDALZAHER (Senior Member, IEEE) received the B.Sc. degree (Hons.) in electronics and communications engineering and the M.Sc. degree in electronics and communications engineering from Ain Shams University, Cairo, Egypt, in 2008 and 2012, respectively, and the Ph.D. degree from the Electronics and Communications Engineering Department, Egypt-Japan University of Science and Technology, Madinet Borg Al Arab, Egypt, in 2016.

He was a Special Research Student with Kyushu University, Fukuoka, Japan, from 2015 to 2016. From April 2019 to October 2019, he joined the Center for Japan-Egypt Cooperation in Science and Technology, Kyushu University, where he was a Postdoctoral Researcher. He is currently an Associate Professor with the Seismology Department, National Research Institute of Astronomy and Geophysics, Cairo. His research interests include earthquake engineering, data communication networks, wireless communications, WSNs security, the IoT, and deep learning. He is also a TPC Member of the Vehicular Technology Conference and International Japan-Africa Conference on Electronics, Communications and Computers. He is a Guest Editor of *Energies* journal and *Frontiers in Communications and Networks* journal. He is a Reviewer of the IEEE Internet of Things Journal, IEEE Systems Journal, IEEE Access, *Transactions on Emerging Telecommunications Technologies*, *Applied Soft Computing*, *Journal of Ambient Intelligence and Humanized Computing*, and IET journals.